# Precisely Designed Difunctionalized Cyclodextrin Produces a Solid-State Organic Porous Hierarchical Supramolecular Assembly

Dmitri Colesnic, Pedro J Hernando, Lise-marie Chamoreau, Laurent Bouteiller, Mickaël M Ménand, Matthieu Sollogoub

# Precisely Designed Difunctionalized Cyclodextrin Produces a Solid-State Organic Porous Hierarchical Supramolecular Assembly

Dmitri Colesnic,[a] Pedro J. Hernando,[a] Lise-Marie Chamoreau,[a] Laurent Bouteiller,*[a] Mickaël Ménand,*[a] Matthieu Sollogoub*[a]

[a]     Dr. D. Colesnic, Dr. P. J. Hernando, L.-M. Chamoreau, Dr. L. Bouteiller, Dr. M. Ménand, Prof. M. Sollogoub
        Sorbonne Université, CNRS
        Institut Parisien de Chimie Moléculaire (IPCM), UMR 8232
        4 place Jussieu, 75005 Paris, France
        E-mail: laurent.bouteiller@sorbonne-universite.fr, mickael.menand@sorbonne-universite.fr, matthieu.sollogoub@sorbonne-universite.fr
        Supporting information for this article is given via a link at the end of the document

**Abstract:** Regioselective di-functionalization of a cyclodextrin allows hydrophobic domains to be directed in a geometrically controlled manner. This controlled orientation ultimately gives access to an original hierarchical assembly in the solid state. This assembly spans over three levels of hierarchy which are governed by synergistic host-guest inclusions, directed hydrophobic effect and hydrogen bonding. This combination of interactions precisely positioned in space through regioselective functionalization of a cyclodextrin creates a porous organic architecture.

## Introduction

The solid state of macrocycle-based supramolecular polymers, underestimated compared to their solution state, is currently attracting increasing interest.[1] These assemblies have promising potential considering the properties of their covalent counterparts which in the solid state generate amorphous or ordered porous materials with applications in the fields of gas adsorption/separation,[2] catalysis[3] or even electronics.[4] These polymers, usually based on perfunctionalized macrocycles, are either reticulated through irreversible bonding (mostly amorphous material) or dynamic covalent bonding (crystalline materials) to create mixed porosity combining the crystal voids to the macrocycle cavities.[5] In contrast, the supramolecular approach uses the cavity of the macrocycle to build the supramolecular polymer through host-guest interactions. It leads, in some cases, to compact arrangements reducing the porosity of the crystalline material.[1] However, following the example of hierarchical macroscopic porous materials,[6] the compactness of the global assembly could be tuned using hierarchical supramolecular architectures. Hierarchical self-assembly is a process in which components are brought together in a controlled manner to form a first level of hierarchy which is further used to build the next level of complexity of self-assembly, forming assemblies of assemblies with controlled architecture. In this approach, small molecular bricks contain all the information encoded for the whole structure on a larger scale. For macrocycle-based supramolecular materials, the functions encoding for geometry and electronic informations have to be precisely introduced to fulfill their role. Consequently, the control of the synthetic modification of these macrocycles is mandatory to obtain tailored properties.

Among the available macrocycles qualified for the building of supramolecular polymers,[7] the cyclodextrin platform has been successfully used for this purpose.[8] The grafting of a hydrophobic substituent on the CD has allowed both to form supramolecular polymers in solution[9,10] and in the solid state (Figure 1a).[11] However, none of these structures demonstrated a hierarchical behavior, because only a primary interaction, the inclusion, was induced by the mono-functionalization of the CD. In contrast, we recently described the solid state structure of a di-functionalized CD which leads to a more complex hierarchical assembly. Indeed, using our DIBAL-H regioselective functionalization tool,[12] we prepared a di-azido α-CD **1** for which the crystalline assembly is strikingly different from the one of the singly functionalized mono-azido α-CD.[13] In the crystal, both azido groups participate and trigger the hierarchical arrangement of the assembly through cooperative interactions.[14] The diazido-CD crystallizes into helicoidal chains constituting the *first level* of hierarchy built-up through the inclusion of an azide group inside the cavity of the contiguous CD. Then, another interaction brings inter-chain cohesion through hydrogen bonds between extroverted azide groups of a helix and the hydroxyl groups of the neighboring one, forming a *second level* of hierarchy. The corresponding crystal assembly is highly compact and does not create pores. (Figure 1b)
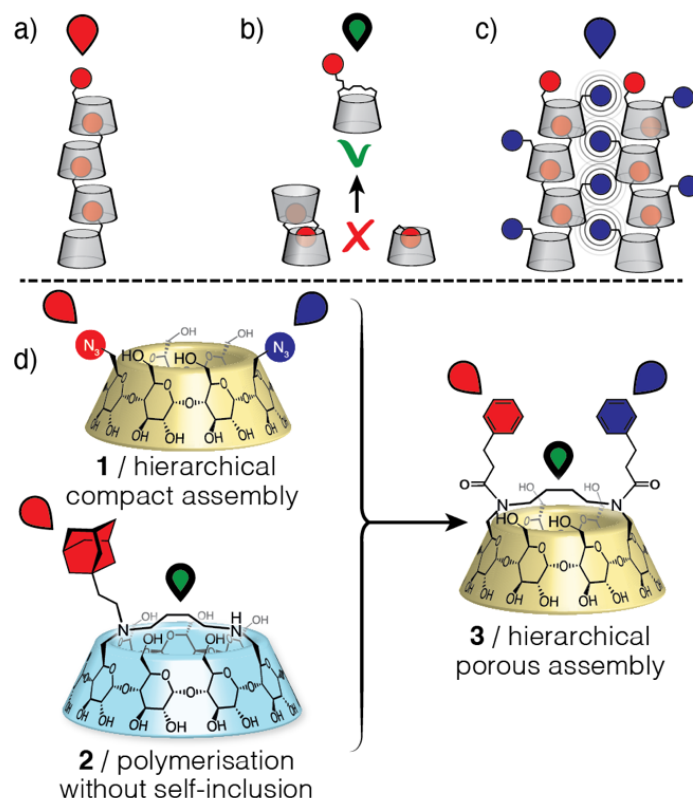
**Figure 1.** Design of the molecular brick **3** using combined strategies derived from compound **1** and **2**, *i.e.* (a) primary assembly through inclusion, (b) bridging to avoid dimerization and/or self-inclusion and (c) secondary side-interactions (d) design of CD **3** combining advantages of CDs **1** and **2**.

We next envisaged to modify the functional groups on the CD to explore different arrangements and possibly obtain pores. As indicated above, difunctionalisation of a CD brings hierarchy to the assembly, but with small $N_3$ groups only compact assemblies were obtained. We thus turned our attention towards the longer hydrocinnamoyl group which was well-studied by Harada.[15] However, attaching a hydrophobic component on top of a hydrophobic cavity can lead to different inclusion complexes together with the desired head-to-tail supramolecular polymerisation: intramolecular self-inclusion, or intermolecular head-to-head oligomerization. To solve this problem, we previously showed that bridging the CD as in CD **2** could avoid self-inclusion and head-to-head oligomerization only leading to its polymerization (Figure 1c).[16] We thus decided to combine both strategies through the grafting of two hydrocinnamoyl groups on a bridged CD **3** (Figure 1d). The two hydrophobic aryl groups were selected to have different roles: one to form an inclusion complex, the other to produce a secondary interaction through $\pi-\pi$ interactions and/or hydrophobic effect. We therefore describe herein the synthesis of this difunctionalized bridged $\alpha$-CD derivative **3** which assembles in the solid state into columnar supramolecular polymers, that further assemble over two additional levels of hierarchy that promote the formation of pores.

## Results and Discussion

The synthesis started with the perbenzylation of the native α-CD, followed by the selective debenzylation reaction in the presence of DIBAL-H, to give diol **4**, with a yield over 80% in two steps.[12] Then the diol **4** was oxidized using Dess-Martin periodinane to give the corresponding dialdehyde which was directly engaged in a reductive amination reaction with 1,4-diaminobutane, to obtain the bridged compound **5** with a yield of 58% over two steps. The obtained diamine **5** underwent a coupling reaction with trans-cinnamic acid, in the presence of coupling agents (EDCI, HOBt) in 55% yield. Compound **6** finally underwent a hydrogenolysis reaction to give the desired CD **3** in 71% yield (Scheme 1).

The di-amide CD **3** is hardly soluble in water reaching saturation at a concentration of less than 0.5 mM. As a result, slow evaporation of water afforded small crystalline needles of compound **3**.[17] The XRD analysis of one of these needles showed a single CD in the unit cell (Figure 2a,b). The CD torus is slightly distorted by the butyl bridge adopting a gauche conformation which slightly tilts the two bridged glucose units A and D (Figure 2c). Moreover, the $^4C_1$ conformation of all the glucose units and the intramolecular hydrogen bonding network between the secondary hydroxyl groups (C2-OH and C3-OH) are preserved. All these features stabilize the CD torus conformation with a well-defined cavity. Furthermore, the

two phenyl groups connected to the bridge adopt a dissymmetrical conformation which contrasts with the $C_2$ symmetric behavior in solution (NMR spectra, see SI).
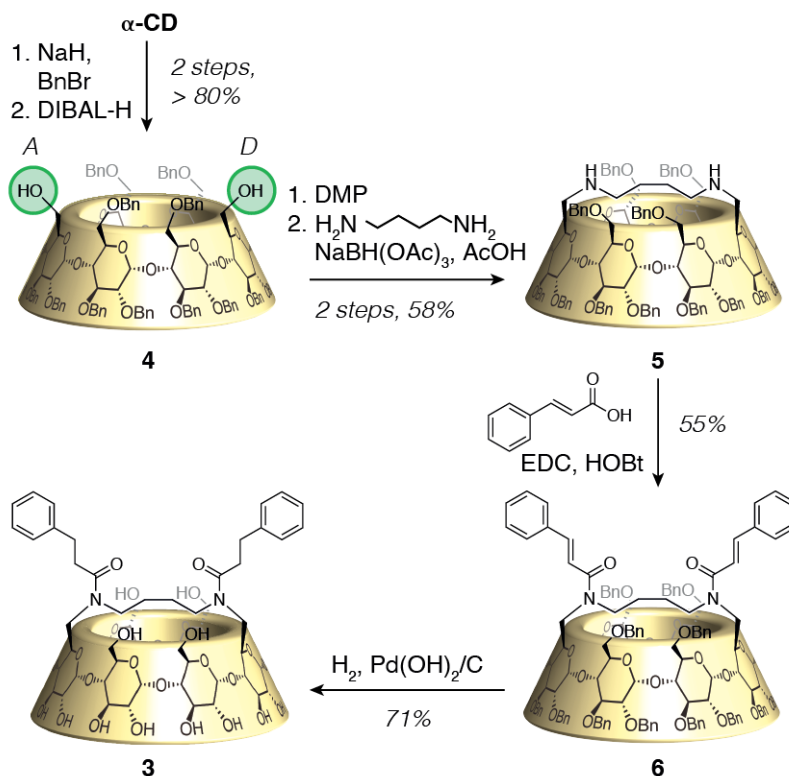


**Scheme 1.** Synthesis of diamide compound **3** *via* peptide coupling.

Indeed, despite both amide bonds display $C_2$ symmetrical arrangement (Figure 2d), the two phenyl rings are arranged in a very different way: the first one (phenyl A) folds its spacer to locate the phenyl ring on the axis of the CD while the second one (phenyl D) is spread out, perpendicular to the axis of the CD, and shows some disorder indicating several possible orientations. Looking at the arrangement of the CD in the packing further reveals the formation of an inclusion complex with the phenyl A partly included in the cavity of another CD (Figure 3a). The dimer is efficiently stabilized by three hydrogen bonds involving the carbonyl groups of the amide bonds and the hydroxyl groups of the secondary rims ($d_{COA\cdots O3C}$ = 2.63 Å, $d_{COD\cdots O2D}$ = 2.78 Å and $d_{OD\cdots O3D}$ = 2.89 Å, Figure 3b). In addition, 7 water molecules strengthen the host-guest interaction acting as a hydrogen bonding relay between the hydroxyl groups (OH-6) of the primary ring and those (OH-2 and OH-3) of the secondary ring (Figure 3b). The repeated inclusion complex (each 10.1 Å) in synergy with the water molecules provide the central backbone forming a rod-like supramolecular polymer (Figure 3a).
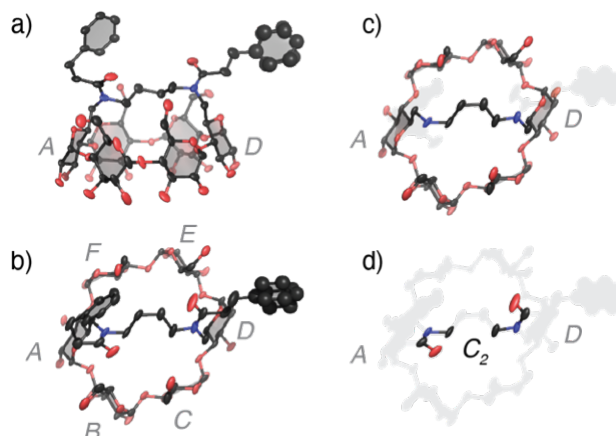


**Figure 2.** X-ray structure (ellipsoid representations, hydrogens and water omitted) of CD **3** view from (a) the side and (b) the top. Details of (c) the bridged CD torus and (d) the $C_2$ symmetrical arrangement of the amide bonds.
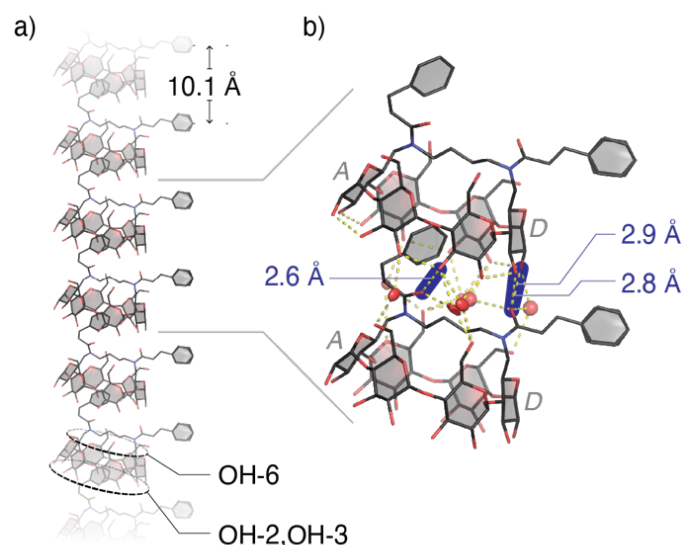
**Figure 3.** *First hierarchical level.* (a) Columnar supramolecular polymer obtained by primary host-guest interaction (water omitted); (b) Inclusion complex dimer showing the hydrogen bonding network between two CDs and the 7 water molecules (the hydrogen bonds between the amide carbonyl groups and the secondary hydroxyl groups are highlighted in blue).

At this stage, the di-functionalized CD **3** behaves broadly like other monosubstituted CDs forming columnar assemblies. However, while the first phenyl (A) provides linear assembly, the second phenyl (D) adds a lateral interaction allowing the assembled columns to behave as advanced building blocks for the construction of higher hierarchy levels. Indeed, the single sided piling of the lateral phenyl groups along the columnar assembly delineates a clear hydrophobic direction (Figure 3d). A shifted arrangement is observed between two neighboring strands (5.4 Å, Figure 4a, 4d) which allows to combine the piled phenyl groups in an original zipper-like fashion strengthening the hydrophobicity (Figure 4a). Furthermore, the arrangement of the zipped phenyl rings allows to recruit four additional strands in an hexameric assembly (Figure 4b). This latter encloses the lateral phenyl rings into an hexagonal channel which expels water molecules out of the formed hydrophobic domain (Figure 4c). Following the offset of the supramolecular polymer strands within the hexamer, the central phenyl groups are arranged into alternating storeys of trimers (Figure 4d). For a given storey, the distances between the barycenters of the three phenyl rings are 5.4 Å in agreement with the molecular distances in liquid benzene and toluene (5.75 Å).[18] Due to the three-fold symmetry, the angle between the average planes of the phenyl's disordered carbon atoms is 62° which is poorly efficient for aromatic interactions as parallel displaced and T-shaped stacking give the most favorable electrostatic interactions.[19] Meanwhile, water exclusion from the phenyl-rich domain indicates that solvation effects may be energetically dominant and that the columnar hexamer is probably governed by the hydrophobic effect[20] rather than by $\pi$-$\pi$ interactions. Hence, as in the case of the di-azido CD previously described,[14] the presence of a second function triggers the second level of hierarchy which otherwise is not observed for mono-functionalized CDs. In addition to the hydrophobic interaction, the individual columnar assemblies are also interacting with neighboring assemblies through a hydrogen bonding network involving the glucose units C, D, E and F (Figure 5a). The "sticky" association is either achieved by direct hydroxyl bonding ($d_{O6C\cdots O2E}$ = 2.6 Å, $d_{O3D\cdots O5E}$ = 3.2 Å and $d_{O3D\cdots O6E}$ = 2.8 Å) or through a relay with a water molecule ($d_{O1W\cdots O2E}$ = 2.9 Å , $d_{O1W\cdots O3E}$ = 2.7 Å, $d_{O1W\cdots O6F}$ = 2.7 Å and $d_{O1W\cdots O5D}$ = 2.9 Å). The inter-strand hydrogen bonding network is made possible by the shift in the alignment of the CD sequence of each strand also necessary to the phenyl group zipping (Figure 5b). The 5.4 Å shift allows for a fine steric matching of the neighboring strands and this self-complementarity allows the strands to achieve very close proximity.
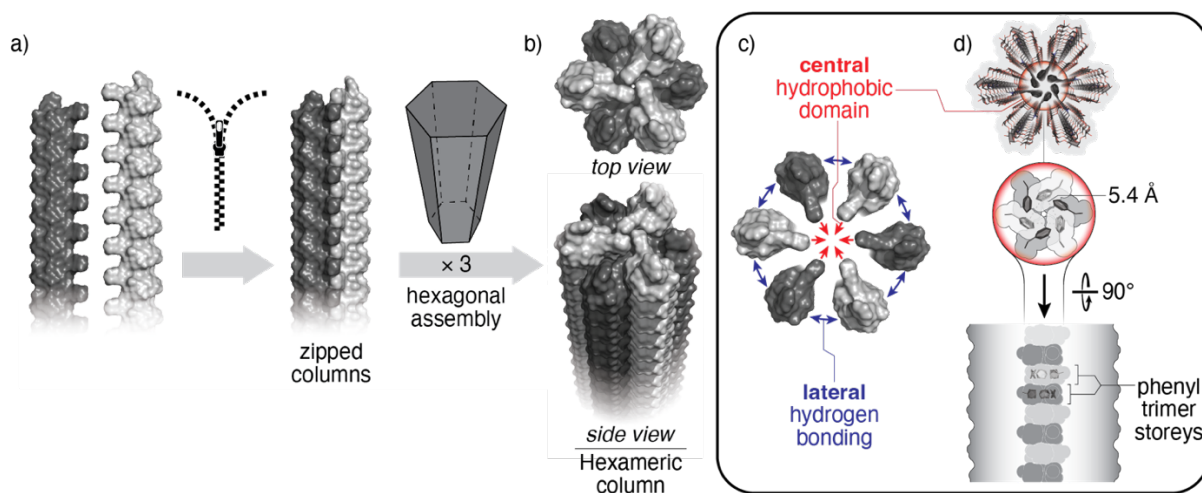
**Figure 4.** *Second hierarchical level*. (a) Zipper-like interlocking of neighboring supramolecular polymers. (b) Top and side views of the hexagonal assembly of supramolecular polymers. (c) Top view (surface representation) of the hexameric superstructure highlighting the interactions responsible for the assembly. (d) Top and side views (stick representations within the columnar volume of the central hydrophobic domain showing the alternating storeys of the disordered phenyl trimers and the distance between two barycenters (top view in the red circle).
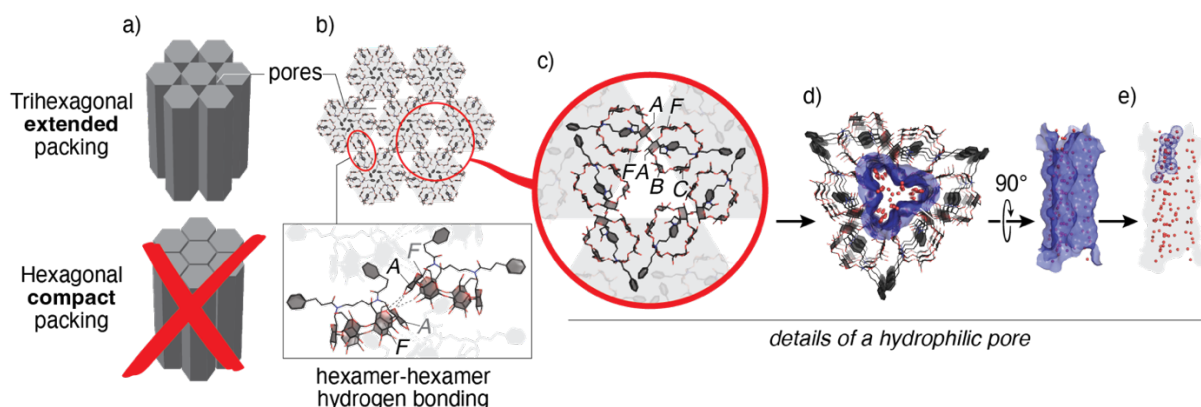


**Figure 5.** *Third hierarchical level creates the pores.* (a) Cartoon representation comparing hexagonal and trihexagonal packing. (b) Trihexagonal packing of the hexameric columns (stick view from the primary rim) and (inset) side view of the hexamer-hexamer hydrogen bonding network. (c) Zoom-in towards the triangular pores. (d) Top and side views of the Connolly surface of the hydrophilic pores. (e) side view of the water molecules within the pore volume (the 13 asymmetric water molecules are highlighted in blue).

Remarkably, changing the azido groups for hydrocynnamoyls induced a drastic change of the mode of assembly, from intertwined helices to hexameric straight rods. However, at this scale, both assemblies are compact and the increase of the size of the arm did not produce any pore. However, the analysis of the crystal packing reveals a third level of organization between the hexameric columns. Indeed, instead of observing an expected compact hexagonal packing, the hexameric columns arrange in an extended trihexagonal packing, resulting in triangular pores intercalated between the hexameric columns and occupying 17% of the volume of the assembly (Figure 5c-e and SI). The triangular pores are formed by connection of the hexameric columns edges through weak hydrogen bonding networks between CDs glucose units A and F (Figure 5b,c; $d_{O5F\cdots O2A}$ = 3.6 Å, $d_{O2F\cdots O5A}$ = 3.2 Å and $d_{O3A\cdots O5A}$ = 3.2 Å). The walls of the corresponding triangular pores are carpeted with hydroxyl groups (glucose units A, B, C and F) which offer a rich interacting site for the non-participating water molecules that are mainly disordered (Figure 5d,e). The triangular pores are not only geometrically complementary with the hexagonal columns, but they are also electronically complementary as they provide hydrophilic domains hosting the free water molecules that are otherwise expelled from the hydrophobic hexameric columns. The stability of the crystalline was assessed by XRD and proved stable at ambient conditions up to two days (See SI). Furthermore, a TGA experiment was performed showing weight loss that is likely due to loss of water in the pores. (See SI)

The solid state structure of monomer **3** provides a striking example of the influence of the functionalization degree of CDs towards the complexity of hierarchical supramolecular self-assembly. This behavior, made possible through the precise introduction of functional groups, is due to both hydrophobic and hydrogen-bonding encoding at the molecular scale (Figure 6a,b). Indeed, the hydrophobic interactions are encoded in the two phenyl rings and the cavity of the CD. The axial

complementarity between phenyl-A and the cavity brings axial directionality and leads to the first level of hierarchy that is supramolecular polymerization. The phenyl-D brings lateral directionality and leads to the second level of hierarchy forming hexameric columns of supramolecular polymers. These two levels are cooperatively assisted by specific hydrogen bonding networks involving water relays. Furthermore, the glucose units act in pairs to encode for specific part of the solid state-assembly. Hence, units E and D are mainly involved in the inter-strand interactions within the hexameric supramolecular polymers ($2^{nd}$ level of hierarchy). Units A and F act as connectors between edges of the hexameric columns ($3^{rd}$ level of hierarchy) and units B and C provides interactions within the hydrophilic pores hosting the residual water molecules. The expression of all the encoded interactions affords the unprecedented three-level hierarchical porous assembly (Figure 6c).
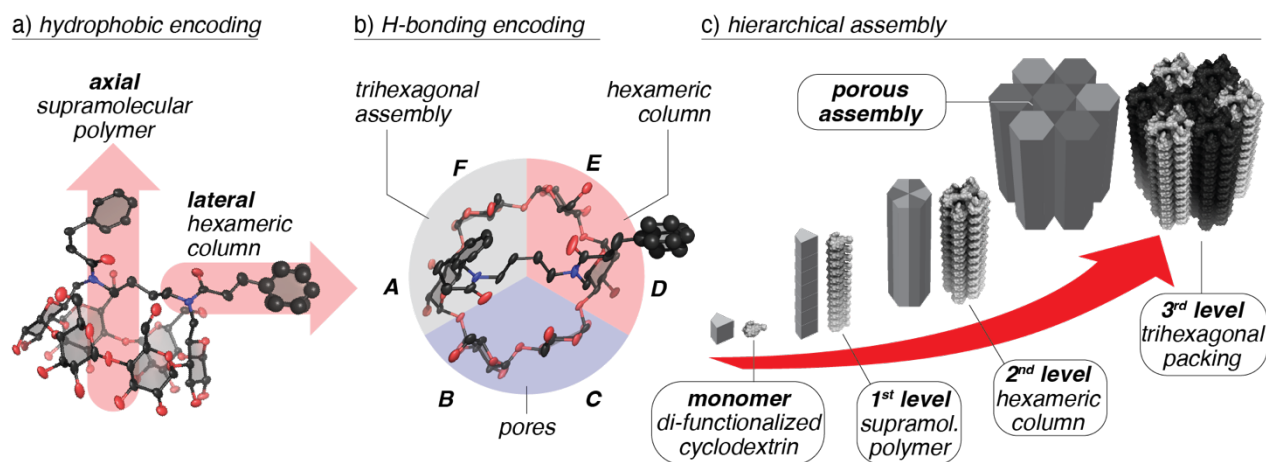


**Figure 6.** Summary of the hierarchical supramolecular assembly : (a) roles of the phenyl rings in the hydrophobic interactions; (b) roles of the glucose units in the hydrogen bonding networks; (c) summary of the different hierarchical levels.

## Conclusion

In conclusion, we demonstrate here that precise functionalization of a macrocyclic structure, CD, allows the control of the architecture of an assembly with a three levels of hierarchy. It has been previously shown that mono-functional CDs gave simple assemblies, while difunctionalized ones afforded hierarchy. Now, this hierarchy was tuned, brought to a higher level of complexity and even produced pores. We now need to study the ability of the pores to accommodate different guests and the possibility to improve this assembly, to make larger pores or different architectures, for example 2D crystals, by exploring other complementary interactions. Indeed, while we only used hydrophobic interactions and H-bonding here, there is a large panel of other weak interactions such as electrostatic interactions or coordination. Their combinations will allow to create more complex and functional solid state of macrocycle-based supramolecular polymers.

## Experimental Section

Crystal data of **3**·11$H_2O$: Colorless needles. $C_{58}H_{104}N_2O_{41}$, $M$ = 1485.43, hexagonal, P $6_3$, $a = b$ = 35.3840(6), $c$ = 10.0824(2) Å $V$ = 10932.2(4) Å$^3$, $T$ = 150 K, space group, $Z$ = 6, 12739 reflections measured ($R_{int}$ = 0.033). Final R factors R1(I>2σ(I)) = 0.0713, w$R2$(all data)= 0.2032.

## Acknowledgements

**Keywords:** Cyclodextrin • Self-assembly • Supramolecular polymer • Hierarchical assembly • Solid state

1    B. Hua, L. Shao, M. Li, H. Liang, F. Huang, *Acc. Chem. Res.* **2022**, DOI 10.1021/acs.accounts.2c00011.

2    See for example : a) N. B. McKeown, B. Gahnem, K. J. Msayib, P. M. Budd, C. E. Tattershall, K. Mahmood, S. Tan, D. Book, H. W. Langmi, A. Walton, *Angew. Chem., Int. Ed.* **2006**, *45*, 1804; b) X. Han, L. Li, Z. Huang, J. Liu, Q. Zheng, *Chin. J. Chem.* **2013**, *31*, 617.

3    See for example : a) H. Li, B. Meng, S.-H. Chai, H. Liu, S. Dai, *Chem. Sci.* **2016**, *7*, 905; b) Z. Li, X. Li, Y.-W. Yang, *Small* **2019**, *15*, 1805509.

4    See for example : Y. Du, H. Yang, J. M. Whiteley, S. Wan, Y. Jin, S.-H. Lee, W. Zhang, *Angew. Chem., Int. Ed.* **2016**, *55*, 1737.

5    a) A. Giri, A. Sahoo, T. K. Dutta, A. Patra, *ACS Omega* **2020**, *5*, 28413–28424; b) W. Chen, P. Chen, G. Zhang, G. Xing, Y. Feng, Y.-W. Yang, L. Chen, *Chem. Soc. Rev.* **2021**, *50*, 11684; c) Z. Li, Y.-W. Yang, *Adv. Mater.* **2022**, *34*, 2107401.

6    X.-Y. Yang, L.-H. Chen, Y. Li, J. C. Rooke, C. Sanchez, B.-L. Su, *Chem. Soc. Rev.* **2017**, *46*, 481–558.

7    S. Dong, B. Zheng, F. Wang, F. Huang, *Acc. Chem. Res*. **2014**, *47*, 1982.

8    Selected examples: A. Harada, Y. Takashima, H. Yamaguchi, *Chem. Soc. Rev.* **2009**, *38*, 875; Y. Chen, Y. Liu, *Chem. Soc. Rev.* **2010**, *39*, 495; G. Chen, M. Jiang, *Chem. Soc. Rev.* **2011**,*40*, 2254; Z. Liu, J. F. Stoddart, *Pure Appl. Chem.* **2014**, *86*, 1323 ; B. V. K. J. Schmidt, C. Barner-Kowollik, *Angew. Chem. Int. Ed.* **2017**, *56*, 8350 ; R. Bleta, A. Ponchel, E. Monflier, *Environ. Chem. Lett.* **2018**, *16*, 1393.

9    For a review see: (a) A. Harada, Y. Takashima, H. Yamaguchi, *Chem. Soc. Rev.* **2009**, *38*, 875 ; (b) A. Harada, A. Hashidzume, *Aust. J. Chem.* **2010**, *63*, 599.

10   S. Dong, B. Zheng, F. Wang, F. Huang, *Acc. Chem. Res.* **2014**, *47*, 1982.

11   K. Hirotsu, T. Higuchi, K. Fujita, T. Ueda, A. Shinoda, T. Imoto, I. Tabushi, *J. Org. Chem.* **1982**, *47*, 1143; S. Kamitori, K. Hirotsu, T. Higuchi, K. Fujita, H. Yamamura, T. Imoto, I. Tabushi, *J. Chem. Soc., Perkin Trans. 2*, **1987**, 7; K. Harata, *Chem. Rev.* **1998**, *98*,1803; Y. Liu, C.-C. You, M. Zhang, L.-H. Weng, T. Wada, Y. Inoue, *Org. Lett.* **2000**, *2*, 2761; K. Harata, Y. Takenaka, N. Yoshida, *J. Chem. Soc., Perkin Trans. 2* **2001**, 1667; Y. Liu, Z. Fan, H.-Y. Zhang, C.-H. Diao, *Org. Lett.* **2003**, *5*, 251; V. H. S. Tellini, A ; . Jover, L. Galantini, F. Meijide, J. V. Tato, *Acta Crystallogr. Sect. B* **2004**, *60*, 204; Y. Liu, Y. L. Zhao, H. Y. Zhang, E. C. Yang, X. D. Guan, *J. Org. Chem.* **2004**, *69*, 3383.

12   a) T. Lecourt, A. Hérault, A. J. Pearce, M. Sollogoub, P. Sinaÿ, *Chem. Eur. J.* **2004**, *10*, 2960 ; b) O. Bistri, P. Sinaÿ, M. Sollogoub, *Tetrahedron Lett.* **2005**, *46*, 7757 ; c) O. Bistri, P. Sinaÿ, M. Sollogoub, *Chem. Commun.* **2006**, 1112 ; d) O. Bistri, P. Sinaÿ, J. Jiménez Barbero, M. Sollogoub, *Chem. Eur. J.* **2007**, *13*, 9757 ; e) S. Guieu, M. Sollogoub, *J. Org. Chem.* **2008**, *73*, 2819 ; f) S. Guieu, M. Sollogoub, *Angew. Chem. Int. Ed.* **2008**, *47*, 7060 ; g) E. Zaborova, M. Guitet, G. Prencipe, Y. Blériot, M. Ménand, M. Sollogoub, *Angew. Chem. Int. Ed.* **2013**, *52*, 639 ; h) B. Wang, E. Zaborova, S. Guieu, M. Petrillo, M. Guitet, Y. Blériot, M. Ménand, Y. Zhang, M. Sollogoub *Nature Comms.* **2014**, *5*, 5354.

13   S. Hanessian, A. Benalil, M. Simard, F. Bélanger-Gariépy, *Tetrahedron* **1995**, *51*, 10149

14   M. Ménand, S. Adam de Beaumais, L.-M. Chamoreau, E. Derat, S. Blanchard, Y. Zhang, L. Bouteiller, M. Sollogoub, *Angew. Chem. Int. Ed.* **2014**, *53*, 7238.

15   T. Hoshino, M. Miyauchi, Y. Kawaguchi, H. Yamaguchi, A. Harada, *J. Am. Chem. Soc.* **2000**, *122*, 9876; A. Harada, Y. Kawaguchi, T. Hoshino, *J. Incl. Phenom. Macro.* **2001**, *41*, 115; M. Miyauchi, Y. Kawaguchi, A. Harada, *J. Incl. Phenom. Macro.* **2004**, *50*, 57.

16   P. Evenou, J. Rossignol, G. Pembouong, A. Gothland, D. Colesnic, R. Barbeyron, S. Rudiuk, A.-G. Marcelin, M. Ménand, D. Baigl, V. Calvez, L. Bouteiller, M. Sollogoub, *Angew. Chem. Int. Ed.* **2018**, *57*, 7753.

17   Crystal data of **3**•11H2O: Colorless needles. C58H104N2O41, *M* = 1485.43, hexagonal, P 63, *a* = *b* = 35.3840(6), *c* = 10.0824(2) Å *V* = 10932.2(4) Å3, *T* = 150 K, space group, *Z* = 6, 12739 reflections measured (*R*int = 0.033). Final R factors R1(I>2σ(I)) = 0.0713, w*R2(all data)*= 0.2032.

18   T. F. Headen, C. A. Howard, N. T. Skipper, M. A. Wilkinson, D. T. Bowron, A. K. Soper, *J. Am. Chem. Soc*. **2010**, *132*, 5735.

19   C. A Hunter, J. K. M. Sanders, *J. Am. Chem. Soc*. **1990**, *112*, 5525.

20   C. R. Martinez, B. L. Iverson, *Chem. Sci*. **2012**, *3*, 2191.